Green Chemistry

Accepted Manuscript

This article can be cited before page numbers have been issued, to do this please use: W. guo, H. Liu, S. Zhang, H. Han, H. Liu, T. Jiang, B. Han and T. Wu, *Green Chem.*, 2016, DOI: 10.1039/C6GC02630C.

ROYAL SOCIETY OF CHEMISTRY

www.rsc.org/greenchem

View Article Online
DOI: 10.1039/C6GC02630C

Journal Name

ARTICLE

Efficient Hydrogenolysis of 5-Hydroxymethylfurfural to 2,5-Dimethylfuran over Cobalt and Copper Bimetallic Catalyst on N-Graphene-Modified Al_2O_3

Received 00th January 20xx,
Accepted 00th January 20xx

DOI: 10.1039/x0xx00000x

www.rsc.org/

Weiwei Guo[ab], Hangyu Liu[ab], Suqi Zhang[a], Hongling Han[ab], Huizhen Liu*[ab], Tao Jiang*[a], Buxing Han[ab], Tianbin Wu[a]

ABSTRACT: 2,5-Dimethylfuran (DMF) is an important candidate for liquid fuels and can be produced from biomass derived 5-hydroxymethylfurfural (HMF). Efficient transformation of HMF to DMF has not been achieved over non-noble catalyst under milder conditions. Herein, we developed copper and cobalt bimetallic nanoparticle catalyst supported on N-graphene-modified Al_2O_3 (CuCo®/NGr/α-Al_2O_3). It was found that the CuCo®/NGr/α-Al_2O_3 could catalyze the conversion of HMF to DMF effectively and the yield of DMF could reach 99%. The catalyst was completely not active for the hydrogenation of the C=C bond in furan and thus no 2,5-bis(hydroxymethyl), tetrahydrofuran(DHTHF) and 2,5-dimethyltetrahydrofuran (DMTHF) were detected.

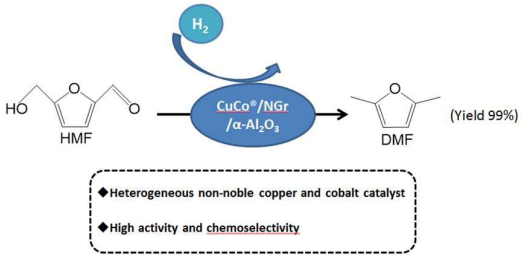

Introduction

The production of liquid fuels directly from biomass is of major interest to reduce dependence on fossil fuel sources. 2, 5-Dimethylfuran (DMF) has been identified as a highly interesting biomass-derived liquid fuels with high energy densities (30 kJ cm^{-3}) and octane numbers (RON = 119), holding great potential to substitute for petroleum-based gasoline.[1,2] On the other hand, as a diene, DMF can also be converted to valuable benzene-based chemicals via Diels–Alder reactions.[3,4]

Production of DMF from the hydrogenolysis of 5-hydroxymethylfurfural (HMF) is a sustainable route that HMF can be produced directly from renewable cellulose.[5] However, HMF hydrogenolysis can produce various products such as 5-methylfurfura (5-MF), 5-methylfurfurylalcohol (5-MFA), 2,5-dimethylfuran (DMF), 2,5-bis(hydroxymethyl)furan (BHMF), 2,5-bis(hydroxymethyl)tetrahydrofuran (DHTHF), 2,5-dimethyltetrahydrofuran (DMTHF) (Scheme 1)，so achieving high yields of DMF in this reaction is a substantial challenge. Noble metal catalyzed the hydrogenolysis of HMF have been studied widely. Gold sub-nano clusters were used to catalyze the selective hydrogenation of HMF, while the product was BHMF.[6] Zu et al. got 93.4% yield of DMF over Ru/Co_3O_4 catalyst in tetrahydrofuran (THF) after 24 h.[7] Wang et al. reported the conversion of HMF over PtCo catalyst and 98% yield of DMF was achieved.[8]

The development of transition-metal-catalyzed organic transformations based on the first-row transition metals such as Fe, Co, Ni, and Cu is of importance because of their relatively low cost and toxicity relative to precious metals. Kong et al. found that non-noble Ni-Al_2O_3 catalysts derived from hydrotalcite-like compounds can efficiently and selectively convert HMF into DMF with 91.5% yield at 180 °C after 4h, and they also developed Ni nanoparticle catalyst and the mixture of DMF and DMTHF was obtained.[9] Raney-type Ni catalyst also can catalyze the hydrogenolysis of HMF and the yield of DMF was 88.5%.[10] Catalytic conversion of HMF to DMF

[a] Beijing National Laboratory for Molecular Sciences, CAS Key Laboratory of Colloid and Interface and Thermodynamics, Institute of Chemistry, Chinese Academy of Sciences, Beijing 100190 (P. R. China). E-mail:liuhz@iccas.ac.cn;
[b] University of Chinese Academy of Sciences, Beijing 100049, (P. R. China).
†Electronic Supplementary Information (ESI) available: [optimization of conditions, GC and GC-MS]. See DOI: 10.1039/x0xx00000x

View Article Online
DOI: 10.1039/C6GC02630C

was also achieved over a Cu-doped porous metal oxide in supercritical methanol, while the yield of DMF was only 40% at 290 °C.[11] Panpan Yang et al. used Ni/Co_3O_4 catalyst in the catalytic conversion of HMF to DMF under relatively mild conditions (130 °C, 1.0 MPa), as high as 76% yield of DMF was achieved.[12] G. Bottari et al. found Noble-metal-free copper–zinc nanoalloy was uniquely suited for the highly selective catalytic conversion of HMF. Clean mixtures of DMF and DMTHF with combined product yields up to 97 % were obtained at 200–220 °C using 2-3MPa H_2.[13] Although Cu and Ni catalysts have been developed, the non-noble metal catalysed hydrogenolysis of HMF to DMF still has ample room for development. The activity of the non-noble metal catalyst and the selectivity of DMF should be further improved.

In this work, we developed a new copper and cobalt bimetallic nanoparticle catalyst supported on N-graphene-modified Al_2O_3 ($CuCo^{®}/NGr/\alpha\text{-}Al_2O_3$) which can efficiently catalyze the hydrogenolysis of HMF to DMF, and the yield of DMF can reach above 99% at 180 °C. Although the activity of the copper catalyst supported on N-graphene-modified Al_2O_3 ($Cu^{®}/NGr/\alpha\text{-}Al_2O_3$) was lower, while the presence of copper contributes to the dispersion of cobalt and the main active component was Co^0. And $CuCo^{®}/NGr/\alpha\text{-}Al_2O_3$ catalyst was completely not active for the hydrogenation of the C=C bond in furan that no DHTHF and DMTHF were detected.

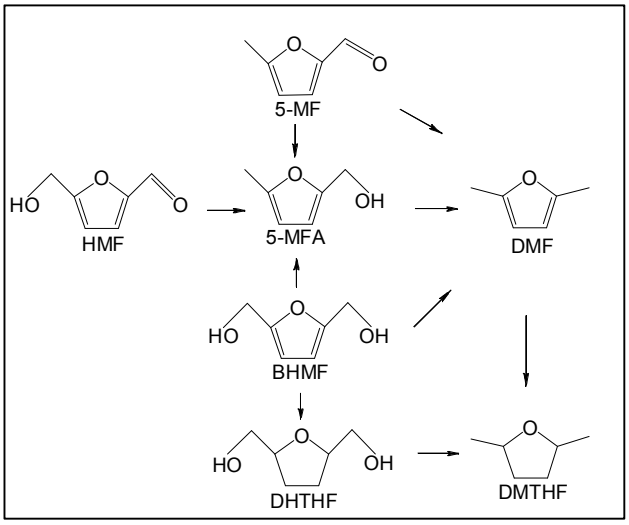

Scheme 1. Conversion of HMF to DMF and other by-products

Experimental

Materials

1,10-Phenanthroline (≥97%), $Cu(OAc)_2$ (≥99%), $Co(OAc)_2{\cdot}4H_2O$ (≥98%), $\alpha\text{-}Al_2O_3$ (≥99.5%) were purchased from Alfa Aesar. Tetrahydrofuran (≥99.5%) was purchased from J&K. 5−Hydroxymethylfurfural (≥98%) was purchased from Sigma-Aldrich. 2,5-Dimethylfuran (97%) was purchased from Polysciences, Inc. All chemicals were used without further purification.

Catalyst preparation

N-graphene-modified $\alpha\text{-}Al_2O_3$ was prepared as following: 1,10-phenanthroline (5.0 mmol) were dissolved in ethanol and then the support $\alpha\text{-}Al_2O_3$ (3.456 g) was added and stirred at room temperature for 24 h. The ethanol was removed under reduced pressure and the sample was dried under vacuum at 60 °C overnight. The solid obtained was ground and calcined for 3 h in a muffle furnace from room temperature to 800 °C with increasing rate of 25 °C/min under argon atmosphere. The catalyst was denoted as $NGr/\alpha\text{-}Al_2O_3$.

$Cu/NGr/\alpha\text{-}Al_2O_3$, $Co/NGr/\alpha\text{-}Al_2O_3$ and $CuCo/NGr/\alpha\text{-}Al_2O_3$ were prepared as described below: the corresponding amount of $Co(OAc)_2{\cdot}4H_2O$ or $Cu(OAc)_2$ or the mixture of $Co(OAc)_2{\cdot}4H_2O$ and $Cu(OAc)_2$ with 1,10-phenanthroline (5.0 mmol) were stirred in ethanol (100 mL) for 15 min at room temperature. Then, the mixture was stirred at 60 °C for 1 h. The support $\alpha\text{-}Al_2O_3$ (3.456 g) was added to the mixture and stirred at room temperature for 24 h. Then, the ethanol was removed under reduced pressure and the sample was dried under vacuum at 60 °C overnight to obtain dark green powder. This solid was ground and calcined for 3 h in a muffle furnace from room temperature to 800 °C with increasing rate of 25 °C/min under argon atmosphere. The solid was grinded a fine powder. If needed, the catalyst obtained was reduced in H_2 at desired temperature for 2 h. The catalyst was reduction by H_2 was denoted as $Cu^{®}/NGr/\alpha\text{-}Al_2O_3$, $Co^{®}/NGr/\alpha\text{-}Al_2O_3$ and $CuCo^{®}/NGr/\alpha\text{-}Al_2O_3$. The ratio of Cu and Co was adjusted by controlling the amount of $Co(OAc)_2{\cdot}4H_2O$ and $Cu(OAc)_2$ added.

Catalyst characterization

The contents of different elements in the catalysts were analyzed by ICP-AES (PROFILE. SPEC, Leeman). Powder X-ray diffraction (XRD) patterns were recorded on a Rigaku D/max-2500 X-ray diffractometer using Cu Kα radiation (λ = 0.15406 nm). The tube voltage was 40 kV and the current was 200 mA. The structural properties were characterized by transmission electron microscopy (TEM, JEOL-2011, JEOL JEM-2100F) and scanning electron microscope (SEM, HitachiS-4800). The X-ray photoelectron spectroscopy (XPS) data were obtained with an ESCA Lab 220i-XL electron spectrometer from VG Scientific using 300 W Al Kα radiations. The base pressure was about 3×10^{-9} mbar. The binding energies were referenced to the C 1s line at 284.8 eV from adventitious carbon.

Catalytic activity tests

The reaction was carried out in a Teflon-lined stainless-steel reactor of 10 mL in capacity with a magnetic stirrer. The pressure was determined by a pressure transducer (FOXBORO/ICT, Model 93), which could be accurate to ±0.025 MPa. In a typical experiment, 1mmol (126 mg) of HMF, 2 mL of solvent and the required amount of catalyst (100 mg) were introduced into the reactor vessel. The reactor was sealed and purged with H_2 to remove the air at ambient temperature. The reactor was placed in an air bath at desired temperature. H_2 of desired pressure was added and then the stirrer was started at

View Article Online
DOI: 10.1039/C6GC02630C

500 rpm. After reaction the reactor was placed in ice water and the gas was released. Finally, the liquid samples were analyzed by a GC (Agilent 6820) equipped with a flame ionization detector. Product identification was done using authentic standards and by using GC-MS that analysis was conducted on Agilent 7890B GC + 5977 MSD.

Results and Discussion

Catalyst Screening and characterization

The hydrogenolysis of HMF over different catalysts was checked and the results are shown in Table 1. α-Al_2O_3 was active for the hydrogenolysis of HMF, and the conversion of HMF was 53.9%. However, the main product was BHMF with 42.3% yield (Table 1, entry 1). The yield of DMF was only 10.2% over NGr (Table 1, entry 2). The conversion of HMF and the yield of DMF increased to 65.7% and 46.2% respectively over NGr/α-Al_2O_3 (Table 1, entry 3). However, the activity of Cu/NGr/α-Al_2O_3 was lower than NGr/α-Al_2O_3 (Table 1, entry 4). Maybe because the coordination of copper and 1,10-phenanthroline changed the chemical state of N-graphene layer and it can be demonstrated by the XPS of N 1s, and it will be discussed below. The activity of Cu®/NGr/α-Al_2O_3 which was reduced by H_2 at 400 °C was better than that of Cu/NGr/α-Al_2O_3 that the conversion of HMF increased to 39.9%, however, the yield of DMF was only 8.0% (Table 1, entry 5). Co/NGr/α-Al_2O_3 exhibited better activity with 85.9% conversion of HMF and 64.1% yield of DMF (Table 1, entry 6). Although the conversion of HMF over Co®/NGr/α-Al_2O_3 which was 97.3% was higher than over Co/NGr/α-Al_2O_3 which was 85.9%, the yield of DMF was similar (Table 1, entries 6-7). Interestingly, although the activity of CuCo/NGr/α-Al_2O_3 was slightly lower than that of Co/NGr/α-Al_2O_3 and Co®/NGr/α-Al_2O_3 (Table 1，entries 6-8), the yield of DMF can reach above 99% over CuCo®/NGr/α-Al_2O_3 (Table 1, entry 10). After 24 h, the yield of DMF also can reach above 99% over CuCo/NGr/α-Al_2O_3 (Table 1, entry 9). However, the yield of HMF was only 62.8% over CuCo®/α-Al_2O_3 which indicated that N-graphene was important for improving the activity of the catalyst (Table 1, entry 11). The ratio of Cu to Co also had an effect on the conversion of HMF and the yield of DMF (Table 1, entries 10, 12 and 13). When the ratio of Cu to Co is 2:1, the conversion of HMF was 73.2% and the yield of DMF was 45.9% (Table 1, entry 12). When the ratio of Cu to Co is 1:2, the conversion of HMF was 81.6% and the yield of DMF was 57.3% (Table 1, entry 13). The above results indicated that although the activity of copper based catalyst was lower, the existence of Cu in the catalyst was important for improving the activity of CuCo®/NGr/α-Al_2O_3 catalyst. In summary, CuCo®/NGr/α-Al_2O_3 with the ratio 1:1 of Cu and Co is exhibited high efficiency for the hydrogenolysis of HMF. The content of the metallic cobalt and copper were identified by ICP. The Co, Cu，N and C content of the most active catalyst (CuCo®/NGr@α-Al_2O_3) was 1.31%, 1.90%, 0.92% and 12.86%, respectively.

Table 1. Effects of different catalysts on the hydrogenolysis of HMF

Entry	Catalysts	Yields (%)					Conv.(%)
		DMF	5-MFA	5-MF	BHMF	others	
1	α-Al_2O_3	1.5	1.4	2.9	42.3	5.9	53.9
2	NGr	10.2	10.7	7.8	0.6	8.1	37.4
3	NGr/α-Al_2O_3	46.2	1.2	2.0	15.7	0.5	65.7
4	Cu/NGr/α-Al_2O_3	2.1	3.4	3.5	11.3	3.2	23.5
5[a]	Cu®/NGr/α-Al_2O_3	8.0	2.4	3.5	17.6	8.4	39.9
6	Co/NGr/α-Al_2O_3	64.1	5.8	3.5	7.0	5.5	85.9
7[a]	Co®/NGr/α-Al_2O_3	65.5	3.0	3.3	3.8	21.7	97.3
8	CuCo/NGr/α-Al_2O_3	63.8	1.1	6.6	3.9	4.2	79.6
9[b]	CuCo/NGr/α-Al_2O_3	>99	0	0	0	0	>99
10[a]	CuCo®/NGr/α-Al_2O_3	>99	0	0	0	0	>99
11[a]	CuCo®/α-Al_2O_3	62.8	0.3	1.5	6.9	11.4	82.8
12[a]	Cu_2Co®/NGr/α-Al_2O_3	45.9	2.6	4.2	17.9	12.5	73.2
13[a]	$CuCo_2$®/NGr/α-Al_2O_3	57.3	0.9	2.0	9.9	11.6	81.6

Reaction conditions: HMF (1 mmol), catalyst (100 mg), P_{H2} (2 MPa), Solvent (THF 2 mL), reaction temperature (180 °C), reaction time (16 h), stirring speed (600 rpm). [a]the catalyst was reduced at 400 °C, [b]reaction time 24 h.

The morphologies of CuCo®/NGr/α-Al_2O_3 were investigated by SEM. Some of their representative images are shown in Fig. 1a-b. The micrographs demonstrated the blocky structure morphology with 200 nm of average crystallite size 20 nm particles was seen from the TEM images (Fig.1c-f). Maybe they were ascribed to metallic Co and Cu. EDS maps of the catalysts (CuCo®/NGr/α-Al_2O_3) indicate the existence of copper, cobalt, aluminum, carbon and nitrogen element on the catalyst (Fig. 2).

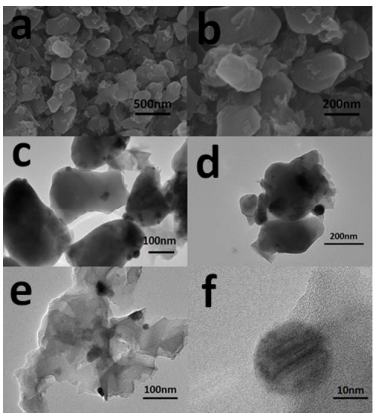

Figure 1. SEM images of CuCo®/NGr/α-Al_2O_3 (a-b), TEM images of CuCo®/NGr/α-Al_2O_3 (c-f).

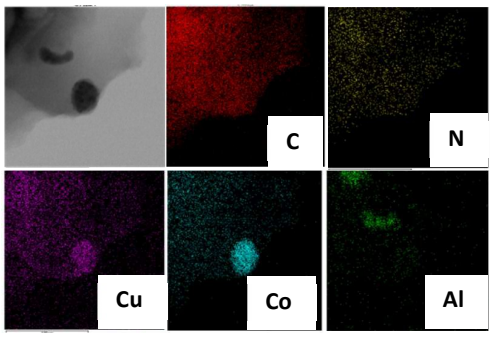

Figure 2. EDS maps of CuCo®/NGr/α-Al_2O_3

View Article Online
DOI: 10.1039/C6GC02630C

To obtain further insight into the chemical composition of this catalyst, X-ray photoelectron spectroscopy (XPS) was performed for the catalyst CuCo/NGr/α-Al_2O_3 and CuCo®/NGr/α-Al_2O_3. As shown in Fig. 3, three peaks are observed in the C 1s spectra of CuCo/NGr/α-Al_2O_3 with electron-binding energy of～284.8 eV, ～286.2eV, and ～288.8 eV (Fig. 3A). In the N 1s XPS spectrum (Fig. 3B), three peaks could be discerned with binding energies at 399.4 eV 401.2 eV, 403.1 eV, assigning to pyridinic, pyrrolic and quaternary nitrogen, respectively for the catalyst CuCo/NGr/α-Al_2O_3.[14] However, the binding energy moved to 399.0 eV, 400.1 eV and 404.3 eV for CuCo®/NGr/α-Al_2O_3 reduced at 400 °C. The decomposed of Co ($2p_{3/2}$) spectrum of specimens containing the distribution of Co^{3+} and of Co^{2+} as well as the Co^{2+} satellite is given in Fig. 4C. The prominent peak around 783.8 eV was assigned to Co^{3+} $2p_{3/2}$ and 780.8 eV was assigned to Co^{2+} $2p_{3/2}$ with its shake up satellite peak at 787.4 was detected for the catalyst CuCo/NGr/α-Al_2O_3 (Fig. 3C (a)).[15-17] The peaks moved of Co^{2+} $2p_{3/2}$ to 781.3 eV, 784.6 eV and 788.0 eV for the catalyst CuCo®/NGr/α-Al_2O_3 (Fig. 3C (b)). The higher binding energy peak at 934.5 eV was assigned to Cu^{2+} in the spinel, accompanied by the characteristic Cu^{2+} shakeup satellite peaks (938–945 eV).[18] The lower binding peak at 932.6 eV for CuCo/NGr/α-Al_2O_3 suggests the presence of Cu^{+} or Cu^{0}. Because $Cu_{2p3/2}$ XPS cannot differentiate between Cu^{+} and Cu^{0}, Auger LMM spectra were used to confirm the presence of Cu^{+} at binding energy 570.7 eV. The binding peaks of Cu^{2+} and Cu^{+} moved to 933.8 eV, 937.8 eV and 932.1 eV, respectively. In summary, the XPS results indicate that the interaction of Cu, Co and N changed for the catalyst before and after reduction that the binding energy was different, although the surface components were all Co^{2+}, Co^{3+} and Cu^{2+}, Cu^{+}.

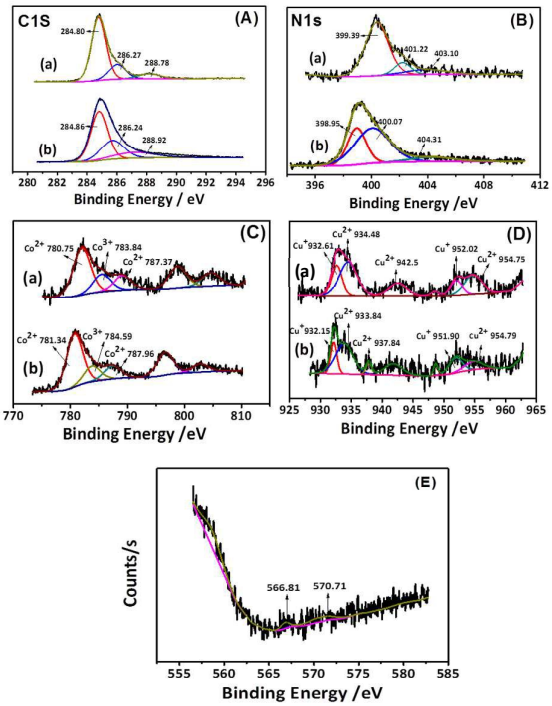

Figure 3. XPS spectrum: (A) C 1s XPS spectra, (B) N 1s XPS spectra, (C) Co $2p_{3/2}$ XPS spectra, (D)Cu $2p_{3/2}$ XPS spectra of (a)CuCo/NGr/α-Al_2O_3, (b) CuCo®/NGr/α-Al_2O_3. (E) AES spectrum of Cu LMM.

The interaction of metal active component and N-Graphene layer were important for improving the activity of the catalyst. The content of different types of C and N on the surface of various catalysts was characterized by X-ray photoelectron spectroscopy (XPS) and the results were shown in Table 2. And the spectrum was shown in Figure S1-S5. For NGr/α-Al_2O_3, the content of pyridinic-N,pyrrolic-N and quaternary nitrogen was 92.1%,3.5% and 4.4%, and changed to 75.5%, 14.3% and 6.6% for Cu/NGr/α-Al_2O_3, respectively (Table 2, entries 1 and 2). Maybe that was the reason of the activity of Cu/NGr/α-Al_2O_3 was lower than NGr/α-Al_2O_3. The content of pyrrolic-N increased from 14.3% to 58.8% for Cu/NGr/α-Al_2O_3 after reduction (Table 2, entry 2 and 3). The content of pyrrolic-N was much higher than other types of nitrogen for Co/NGr/α-Al_2O_3 and Co®/NGr/α-Al_2O_3, and the content of different types of nitrogen didn't changed after reduction. However, for CuCo/NGr/α-Al_2O_3 catalyst, the content of pyrrolic-N increased from 12.8% to 73.7% and of pyrrolic-N decreased from 75.4% to 6.7%. And the yield of DMF increased from 63.8% to >99% for CuCo/NGr/α-Al_2O_3 after reduction. These results indicated that the metal active component and the types of nitrogen influence the activity of the catalyst. The Cu and Co bimetal and pyrrolic-N synergistically promoted the activity of the catalyst. The content of different types of nitrogen changed after reduction that influenced the dispersion of metal on support.

Table 2. The content of different carbon and nitrogen species of the catalyst on the surface

Entry	Catalyst	C1s (%)			N1s (%)		
		Graphene	C–C	C–O	Pyridinic	Pyrrolic	Quaternary Nitrogen
1	NGr/α-Al_2O_3	77.6	14.0	8.5	92.1	3.5	4.4
2	Cu/NGr/α-Al_2O_3	51.9	41.9	6.3	75.5	14.3	6.6
3	Cu®/NGr/α-Al_2O_3	68.8	23.5	7.8	32.4	58.8	8.9
4	Co/NGr/α-Al_2O_3	47.6	42.3	10.1	18.9	68.5	12.6
5	Co®/NGr/α-Al_2O_3	48.8	39.4	11.9	20.3	69.2	10.7
6	CuCo/NGr /α-Al_2O_3	72.0	19.7	8.3	75.4	12.8	11.8
7	CuCo®/NGr /α-Al_2O_3	46.4	43.8	9.9	6.7	73.7	19.6

To investigate the reason of the effect of Cu on the activity of CuCo®/NGr/α-Al_2O_3, the XRD patterns of the catalysts CuCo/NGr/α-Al_2O_3, CuCo®/NGr/α-Al_2O_3, and Co®/NGr/α-Al_2O_3 were adopted (Fig. 4). It is found that CuCo/NGr/α-Al_2O_3 presents the crystalline peaks of Co^{0}、Cu^{0} and Al_2O_3 that indicates that Co and Cu has been reduced to zero valence during the preparation of the catalyst. The peaks at 44.2°, 51.5° and 75.9° corresponded to (111), (200) and (220) reflections of the Co^{0} phase (PDF# 15-0806),[19] while the peaks at 43.2°, 50.4° and 74.1° could be assigned to (111), (200) and (220) planes of the Cu^{0} phase (PDF# 04-0836). The reduction of

View Article Online
DOI: 10.1039/C6GC02630C

CuCo/NGr/α-Al_2O_3 causes the XRD peaks of Co to broaden, while the peaks for Cu^0 did not change (Fig. 4b). The result indicated that the Co was re dispersed on the catalyst surface after reduction in the presence of Cu. And we didn't detect any alloy phase of Cu and Co. The dispersion of the catalyst CuCo/NGr/α-Al_2O_3, CuCo®/NGr/α-Al_2O_3 was 0.1372% and 2.1345% respectively. We can see that the dispersion of metal increased after reduction. Maybe it's one of the reasons of the activity increased.

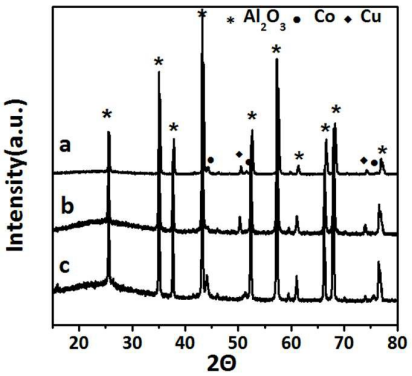

Figure 4. The XRD of CuCo/NGr/α-Al_2O_3(a), CuCo®/NGr/α-Al_2O_3(b), Co®/NGr/α-Al_2O_3(c)

Optimization of the reaction conditions

Effect of reaction temperature and pressure

The influence of reaction temperature and pressure on the HMF hydrogenolysis was studied and the results are shown in Table 3. It can be seen that the temperature played an important role for the reaction (Table 1, entry 9 and table 3, entries 1-4). The conversion of HMF increased from 57.1% to 89.5% and the yield of DMF increased quickly from 21.2% to 72.1% when the temperature increased from 120 °C to 140 °C that indicated that the reaction rate of the byproducts converted to DMF increased more quickly than that of the conversion of HMF (Table 3, entries 1-3). The yield of unidentified products decreased quickly from 120 °C to 140 °C which indicated that these products also can be converted to DMF although they cannot be qualitative (Table 3, entries 2 and 3). The conversion of HMF reached about 100% while the yield of DMF was 83.7% at 160°C (Table 3, entry 4). >99% conversion of HMF and >99% yield of HMF can be reached at 180 °C (Table 1, entry 9).

The influence of reaction pressure on HMF conversion and DMF yield over the catalyst was also investigated (Table 3, entry 5-8). It can be seen that HMF conversion all can reach >99%, while the yield of DMF increased with increasing H_2 pressure. When the H_2 pressure was 1 MPa, the yield of DMF was 77.3%, when the H_2 pressure was above 2 MPa, the yield of DMF all can reach >99%.

Table 3. The effect of reaction temperature and pressure.

Entry	T(°C)	P(H_2) (MPa)	Yields (%)					Conv. (%)
			DMF	5-MFA	5-MF	BHMF	others	
1	100	2	8.1	2.4	5.2	8.7	12.3	36.7
2	120	2	21.2	5.3	6.5	6.9	17.2	57.1
3	140	2	72.1	1.0	2.3	5.4	8.7	89.5
4	160	2	83.7	trace	2.1	4.9	9.3	100
5	180	1	77.3	2.6	4.1	6.4	8.6	99.0
6	180	1.5	89.9	1.3	1.8	3.2	3.8	>99
7	180	2.5	>99	trace	trace	trace	trace	>99
8	180	3	>99	trace	trace	trace	trace	>99

Reaction conditions: HMF (1 mmol), catalyst (100 mg), solvent (THF, 2 mL), stirring speed (600 rpm). Others indicated unidentified products.

Effect of reaction time

The results of the influence of reaction time are shown in Fig. 5. The conversion of HMF and the yield of DMF increased with time. And all the yield of byproducts decreased with time. The yield of BHMF increased with time and then decreased. The results indicate that the hydrogenolysis of HMF is consecutive reaction and the byproducts include the unidentified products can be converted to DMF with time. The highest yield of BHMF was 29.1%. The highest yield of others intermediates were all very low. These results indicated that the conversion of HMF to BHMF is determining step. The DMF also can be further hydrogenation to DMHF, fortunately the catalyst was inactive for the hydrogenation of furan ring and no DMHF product was detected.

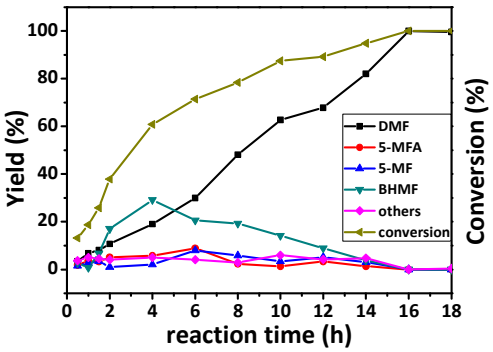

Figure 5. The effect of reaction time. Reaction conditions: HMF (1 mmol), catalyst (100 mg), T (180 °C), solvent (THF, 2 mL), P_{H2} (2 MPa), stirring speed (600 rpm). Others indicated unidentified products

Effect of reaction solvent

The effect of solvent on the catalytic activity in the conversion of HMF to DMF was investigated at the optimum reaction conditions and the results are given in table 4. It can be seen that the catalytic activity in different solvents follows the order: THF>1, 4-dioxane >2-propanol >1- butanol> DMSO>cyclohexanone>H_2O. The strong polar solvent DMSO exhibited the lowest conversion of HMF and yield of DMF (Table 4, entry 1). The conversion of HMF and the yield of DMF were similar in protonic solvent 2-propanol and 1-butanol (Table 2, entries 2 and 3). The catalytic activity in 1, 4-dioxane was better than in DMSO, 2-propanol and 1-butanol that the

View Article Online
DOI: 10.1039/C6GC02630C

conversion of HMF was above 99% and the yield of DMF was 90.1%. THF was the best solvent among the solvent checked with above 99% conversion and above 99% yield of DMF. However, the conversion of HMF and the yield of DMF were very low in nonpolar solvent cyclohexane (Table 4, entry 6). H_2O was also not a good solvent for this reaction maybe because the solubility of the reactant and product (Table 4, entry 7).

Table 4. The effect of different solvents on the hydrogenalysis of HMF

Entry	reaction solvents	Yields (%)					Conv. (%)
		DMF	5-MFA	5-MF	BHMF	others[a]	
1	DMSO	49.8	5.4	7.9	7.2	8.8	79.1
2	2-propanol	67.6	2.5	4.2	7.8	10.3	92.4
3	1-butanol	66.7	3.3	5..6	9.1	11.9	96.6
4	1,4-dioxane	90.1	1.3	1.9	2.7	3.2	>99
5	THF	>99	0	0	0	0	>99
6	cyclohexane	4.9	1.5	1.7	2.8	2.7	13.5
7	H_2O	1.1	12.3	1.3	1.6	0.4	16.7

Reaction conditions: HMF (1 mmol), catalyst (100 mg), T (180 °C), P_{H2} (2 MPa), t (16 h), stirring speed (600 rpm). [a]others indicated unidentified products.

Catalyst recyclability

The reusability of CuCo®/NGr/α-Al_2O_3 catalyst was tested for the hydrogenolysis of HMF to DMF. After the reaction, the reaction mixture was centrifuged and the solid CuCo®/NGr/α-Al_2O_3 catalyst was recovered, followed by rinsing with THF and centrifugation (5×20 mL). The CuCo®/NGr/α-Al_2O_3 catalyst was reused directly for the next run after drying at 80 °C for 6 h in a vacuum oven. The results in Figure 6 clearly showed that the catalytic performance decreased after being reused for five times. By XPS characterization (Figure S6), the content of pyrrolic-N decreased from 73.7% to 60.5% after being reused one time, maybe it was the main reason of the activity of the catalyst decreased.

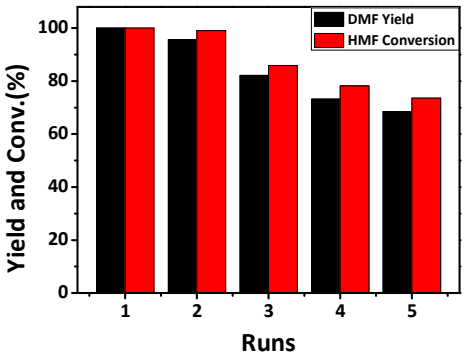

Figure 6. Recyclability experiments with CuCo®/NGr/α-Al_2O_3 catalyst in the hydrogenolysis of HMF to DMF. Reaction conditions: HMF (1 mmol, 126 mg); catalyst (100 mg); reaction temperature (180°C); solvent (THF, 2mL); reaction time (16 h); stirring speed (600 rpm)

Conclusions

CuCo®/NGr/α-Al_2O_3 is very active and selective for the conversion of HMF to DMF, and yield of DMF can be as high as 99% at optimized condition. The main reason for the very high yield is that the catalyst is active for C–O bond cleavage and C=O bond hydrogenation, but is not active for hydrogenation of C=C bond in furan ring, and thus the by-products DHTHF and DMTHF are not produced. The Cu and Co bimetal and pyrrolic-N synergistically promoted the activity of the catalyst. This work provides an effective route for the conversion of HMF to DMF over non-noble metal catalyst.

Acknowledgements

The authors thank the Recruitment Program of Global Youth Experts of China, the National Natural Science Foundation of China (21273253, 21373230) and Chinese Academy of Sciences (KJCX2.YW.H30) for financial supports.

Notes and references

1 Y. R. Leshkov, C. J. Barrett, Z. Y. Liu, J. A. Dumesic, *Nature*, 20 07, 447, 982-985.
2 S. H. Zhong, R. Daniel, H. M. Xu, J. Zhang, D. Turner, M. L. Wyszynski, P. Richards, *Energy Fuels*, 2010, 24, 2891-2899.
3 P.T. M. Do, J. R. McAtee, D. A. Watson, R. F. Lobo, *ACS Catal.*, 2013, 3(1), 41-46.
4 Y. P. Li, M. H. Gordon, A. T. Bell, *J. Phys. Chem. C.*, 2014, 118(38), 22090-22095.
5 J. Ohyama, A. Esaki, Y. Yamamoto, S. Arai, A. Satsuma, *RSC Adv.*, 2013, 3, 1033-1036.
6 M. J. Climent, A. Corma, S. Iborra, *Green Chem.*,2014, 16, 516-547.
7 Y. H. Zu, P. P. Yang, J. J. Wang, X. H. Liu, J. W. Ren, G. Z. Lu, Y. Q. Wang, *Appl.Catal. B: Environ.*, 2014, 146, 244-248.
8 G. H. Wang,J. Hilgert,F. H. Richter,F. Wang,H. Bongard,B. Spliethoff,C. Weidenthaler, F. Schüth, *Nat. Mater.*, 2014, 13, 293-300
9 X. Kong, R. X. Zheng, Y. F. Zhu, G. Q. Ding, Y. L. Zhu, Y. W. Li, *Green Chem.*, 2015, 17, 2504-2514.
10 X. Kong, Y.F. Zhu, H.Y. Zheng, F. Dong, Y.L. Zhu, Y. W. Li, *RSC Adv.*, 2014, 4, 60467-60472.
11 T. S. Hansen, K. Barta, P. T. Anastas, P. C. Ford, A. Riisager, *Green Chem.*, 2012, 14, 2457-2461.
12 P. P. Yang, Q. Q. Cui, Y. H. Zu, X. H. Liu, G. Z. Lu, Y. Q. Wang, *Catal. Commun.*, 2015, 66, 55-59.
13 G. Bottari, A. J. Kumalaputri, K. K. Krawczyk, B. L. Feringa, H. J. Heeres, K. Barta, *ChemSusChem*, 2015, 8, 1 323-1 327.
14 Z. Z. Lin, X. C. Wang, *ChemSusChem*, 2014, 7, 1547-1550.
15 L. Fu, Z. Liu, Y. Liu, B. Han, P. Hu, L. Cao, D. Zhu, *Adv. Mater*, 2005, 17, 217-221.
16 D. X. Yang, T. Jiang, T. B. Wu, P. Zhang, H. L. Han, B. X. Han, *Catal. Sci. Technol.*, 2016, 1 (6), 193-200.
17 B. Ernsta, S. Libsa, P. Chaumetteb, A. Kiennemanna, *Appl. Catal. A*, 1999, 186, 145-168.
18 P. Liu, E. J. M. Hensen, *J. Am. Chem. Soc.*, 2013, 135, 14032-14035.
19 H. C. Zhou, J. L. Song, H. L. Fan, B. B. Zhang, Y. Y. Yang, J. Y. Hu, Q. G. Zhu, B. X. Han, *Green Chem.*, 2014, 16, 3870-3875.